JOURNAL OF SPACECRAFT AND ROCKETS
Vol. 42, No. 2, March–April 2005

Nonequilibrium Viscous Shock-Layer Heat Transfer with Arbitrary Surface Catalycity

George R. Inger*
Iowa State University, Ames, Iowa 50011-2271
and
Richard L. Baker†
The Aerospace Corporation, El Segundo, California 90245-4617

An approximate yet accurate analysis of aerodynamic heating at a highly cooled stagnation region, which embraces the entire high-altitude hypersonic flight regime where nonequilibrium dissociation/recombination in the shock layer and finite surface catalysis effects are both important, is given. Closed-form relationships are given for the relative nonequilibrium effects that are convenient for cost-effective engineering studies of high-altitude hypervelocity vehicle heating.

Nomenclature

C_D, C_E = equilibrium constants; Eqs. (18) and (6), respectively
$\hat{C}_p$ = specific heat of mixture
f_Ω = vorticity functional; Eq. (11)
$f_{1,2,3}$ = density-related functions; Eqs. (7–9)
f_4 = defined in conjunction with Eq. (33)
G = composition-dependent portion of reaction rate; Eq. (18a)
g_z = $I_z(\mathrm{m})/I_z(\mathrm{fe})$; Eq. (27)
H_D = $Le^{0.52}h_D/Cp_S T_S$; Eq. (5)
h_D = specific dissociation energy of molecules
I_D = inviscid reaction carryover effect integral; Eq. (26)
$I_{Z,\theta}$ = viscous-layer integrals; Eq. (24)
$I_{1,2,3}$ = reaction-rate integrals; Eqs. (27) and (28)
K_D = I_D/f_4; Eq. (30)
K_W = speed of catalytic atom recombination on body surface
k_r, k_r' = recombination-rate constants; Eq. (17)
Le = Lewis number, Pr/Sc
M_m = molecular weight of molecules
Pr = Prandtl number
p = static pressure
Q_w = nondimensional heat-transfer rate; Eq. (20)
R = net reaction-rate distribution function; Eqs. (15) and (18)
R_B = nose radius
R_m = molecular gas constant
R_u = universal gas constant
Re_B = $\rho_\infty U_\infty R_B/\propto_\infty$ (Reynolds number)
r = ρ_s/ρ_∞
Sc = Schmidt number
T = absolute temperature
T_D = characteristic dissociation temperature, $= h_D/R_m$
T_F = frozen postshock temperature; Eq. (1)
U_∞ = flight speed
u = chordwise velocity component
Z = nonequilibrium-effect function; Eq. (30)
α = atom mass fraction
β_S = inviscid flow stagnation point velocity gradient, $(\mathrm{d}ue/\mathrm{d}x)s$
Γ_C = Damköhler numbers for surface reaction [Eq. (19)]
$\tilde{\Gamma}_c$ = $\Gamma_c/0.47Sc^{1/3}f_\Omega$
Γ_G = Damköhler number of gas-phase recombination
Γ^* = composite Damköhler number for gas phase and surface reaction; Eq. (31)
ε = 0, 1 for two-dimensional or axisymmetric, respectively
η = boundary-layer similarity coordinate
θ = T/T_e
θ_D = $h_D/R_m T_e$
$\vartheta_{z,\theta}$ = integral function defined by Eq. (25)
λ = viscosity exponent ($\propto \sim T^\lambda$)
ρ = mixture density
τ_R = recombination rate time constant; Eq. (13)
Ω_e = vorticity interaction parameter; Eq. (10)
ω = recombination rate temperature-dependence exponent ($k_r \sim T^\omega$)
$\propto$ = coefficient of viscosity

Subscripts

A = atom
EQ = equilibrium boundary-layer flow
e = nonequilibrium viscous-layer edge conditions
F = frozen viscous flow
M = molecule
REF = standard atmospheric conditions at 300 K; Eq. (13)
SH = location of shock wave
s = inviscid flow conditions at stagnation point (equilibrium)
w = conditions on body surface

I. Introduction

THE aerodynamic heating of hypersonic vehicles at planetary entry speeds is an important aspect of their design and performance analysis. In particular, high-temperature dissociation effects play an important role in this heating. Moreover, owing to the very high flight speeds (short flow residence time) and lower density, high-altitude operating conditions (long chemical reaction collision times), such dissociation effects can be influenced strongly by marked departures from gas-phase chemical equilibrium in the boundary layer combined with finite rates of catalytic atom recombination along the vehicle surface. These nonequilibrium chemistry effects in turn can cause significant reductions in aerodynamic heating, if the body surface is not fully catalytic.[1] Current engineering

Received 13 January 2004; accepted for publication 18 April 2004.

*Professor of Aerospace Engineering. Associate Fellow AIAA.
†Senior Engineering Specialist, Fluid Mechanics Department.

methods for stagnation-point heat-transfer prediction are not fully satisfactory in their treatment of such high-altitude aerothermochemistry, however, because typically they lead to significant overestimates of satellite breakup altitude. It is suspected that the magnitude of the overestimates becomes even greater as the size of the body is decreased. Also, preliminary studies of shallow entry conditions indicate that the resulting multiple-skip entries produce much higher total heat transfer than the usual single-entry values,[2] thereby emphasizing the need for accuracy in the heat transfer predictions.

Altogether, these conclusions suggest the desirability of improving current aerodynamic heating engineering methodology in regard to the physical modeling of the nonequilibrium-dissociation unique to high-altitude hypervelocity flight. In a previous study[3] this need was addressed as concerns the effects of finite recombination-rate chemistry across a stagnation-point boundary layer (the region of maximum heating) in those lower-altitude flight regimes [$\leq$61 km (200 kft)] where the inviscid shock layer outside the boundary layer attains complete dissociative equilibrium. The present paper now takes the work to higher altitudes by providing an extension of Ref. 3 that includes the additional effects of low-Reynolds-number viscous shock-layer behavior and nonequilibrium dissociating flow behind the bow shock. As before, these are presented as closed-form corrections to equilibrium chemistry-assumption results, allowing an arbitrary degree of finite-surface catalycity.

II. Required Input

Because the present analysis provides a fundamentally based "correction" of the combined nonequilibrium dissociation/arbitrary catalycity effects relative to an equilibrium chemistry prediction for the same set of flight conditions, the user is required to have such a baseline equilibrium stagnation heating code or method. Moreover, it is assumed that this baseline code provides two sets of flow property values for each chosen combination of altitude and flight speed U_∞: 1) the ambient static pressure p_∞, density ρ_∞, static absolute temperature T_∞, and coefficient of viscosity $\propto_\infty$; and 2) the equilibrium postshock inviscid stagnation values of density ρ_S, pressure p_S, temperature T_S, and total atom mass fraction α_S. In addition, the user must specify the following physical properties of the flow: the viscosity temperature-dependence exponent $\lambda(\propto \approx T^\lambda, \lambda \approx 0.76)$; values of the Schmidt and Prandtl numbers Sc and Pr, respectively; the gas-phase recombination-rate constant and its temperature-dependence exponent ω (see next); the molecular gas constant R_m and effective heat of dissociation $h_D \equiv T_D \cdot R_m$; the body characteristics including the nose radius R_B, its dimensionality index ε (0 for two-dimensional and 1 for axisymmetric), the wall surface temperature T_W, and the catalytic efficiency parameter γ_C.

With these inputs, the user should generate the following set of key nondimensional parameters needed by the nonequilibrium heat-transfer theory given next (see Nomenclature).

Frozen postshock temperature:

$$T_F = U_\infty^2/9R_m \tag{1}$$

Density ratio:

$$r = \rho_s/\rho_\infty \tag{2}$$

Reynolds number:

$$Re_B = \rho_\infty U_\infty R_B/\propto_\infty \tag{3}$$

Mixture specific heat (fully excited vibration):

$$\hat{C}_p = (9+\alpha_s)R_m/2 \tag{4}$$

Nondimensional dissociation energy parameter:

$$H_D = Le^{0.52} h_D/\hat{C}_p T_s \tag{5}$$

Table 1 Typical catalytic efficiencies of various surface materials at room temperature (oxygen atoms) (from Ref. 4)

Material	$\gamma_A \times 10^4$	Material	$\gamma_A \times 10^4$
Ag	2400	Se	1.7
Cu	1700	CuO	200
Fe	360	NiO	77
Ni	280	Al_2O_3	26
Au	52	Pyrex	1.2
Sb	8.2	KC1	2.8
As	4.6	CsC1	3

Table 2 Typical recombination-rate parameters for dissociated air (averaged values)

$\tau_R \times 10^6$	$\omega(k_r \sim T^\omega)$	Reference
1.10	−1.50	5
2.05	−0.50	6

Equilibrium constant:

$$C_E = \left[\alpha_s^2 (e^{T_D/T_S})\Big/\left(1-\alpha_s^2\right)\right](\theta_D)^{1.5}[1-e^{-\theta_D/\theta}]/[1-e^{\theta_D}] \tag{6}$$

Trio of density-related parameters:

$$f_1 = r\Big/\sqrt{2(r-1)} \tag{7}$$

$$f_2 \equiv \sqrt{f_1 Re_B (T_F/T_\infty)^{1-\lambda} 6(r-1)/(1+\varepsilon)5rp_s/p_\infty} \tag{8}$$

$$f_3 \equiv \sqrt{1+(3.38/f_2)^{2/(1+\varepsilon)}\left(f_1^2-1\right)} \tag{9}$$

Vorticity interaction parameters:

$$\Omega_e = (f_1-1)/2f_2 \tag{10}$$

$$f_\Omega \equiv 1 + 0.50\Omega_e - 0.11\Omega_e^2 \tag{11}$$

Wall catalysis Damköhler number (a characteristic flow time/reaction time ratio):

$$\Gamma_c = 0.475 Sc\gamma_e r \times \sqrt{\frac{R_m T_s}{U_\infty^2}\frac{Re_B}{(1+\varepsilon)}\left(\frac{T_\infty}{T_w}\right)^2 (r-1)^{-\frac{1}{2}}\left(\frac{T_F}{T_w}\right)^{\lambda-1}\frac{5r(1+\alpha_s)}{6(r-1)}} \tag{12}$$

where typical values of γ_C (which is T_W dependent) are to be selected by the user for the particular wall material involved. [See the summary provided in Ref. 3, which is repeated here for convenience in Table 1 (Ref. 4).]

Gas-phase recombination Damköhler number:

$$\Gamma_G \equiv 2.834 Sc\left(\frac{R_B/U_\infty}{\tau_R}\right)\left(\frac{\rho_\infty}{\rho_{\text{REF}}}\right)^2\left(\frac{T_s}{T_{\text{REF}}}\right)^{\varpi}\frac{r^3(1+\alpha_s)^2}{(1+\varepsilon)\sqrt{r-1}} \tag{13}$$

where ρ_{REF} refers to standard atmospheric density at $T_{\text{REF}} = 300$ K and $\tau_R \equiv (k_R' T_{\text{REF}}^\omega \rho_{\text{REF}}^2/M_{\text{m}}^2)^{-1}$ is the recombination-rate time constant appropriate to the reaction-rate data selected by the user. [Typical values are listed here in Table 2 (Refs. 5 and 6).]

III. Analytical Treatment of the Problem

A. Assumptions and Limitations

Our analysis is based on a continuum theory of nonequilibrium-dissociated airflow in the nose region behind the shock envelope, around a highly cooled body (see Fig. 1), under an expanded regime of hypervelocity flight conditions that now includes dissociative

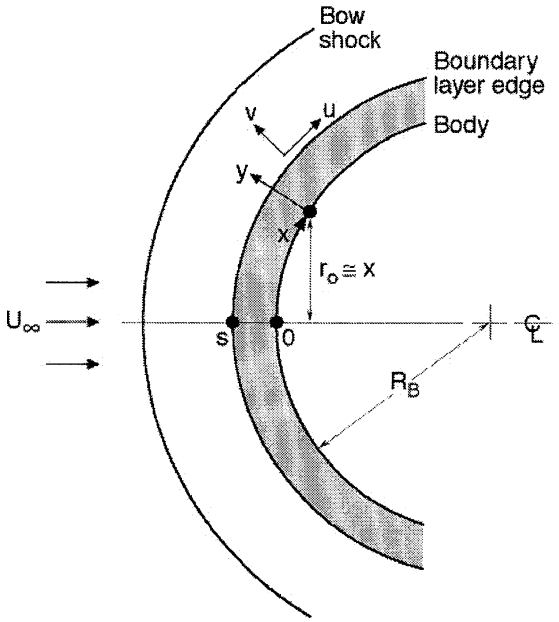

Fig. 1 Stagnation-region flow (schematic).

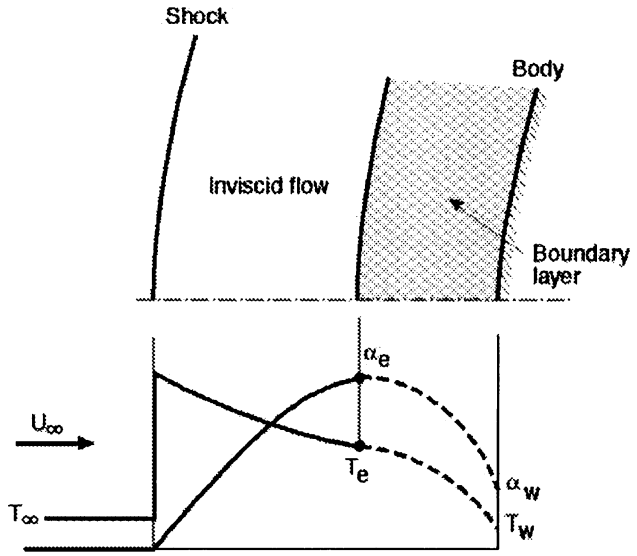

Fig. 2 Nonequilibrium shock layer flow at lower Reynolds numbers (schematic).

nonequilibrium across the outer inviscid portion of the shock layer as well as the nonequilibrium recombination within the underlying boundary layer and body surface. That is, we now additionally embrace the very high-altitude situation above 61–76 km (200–250 kft), where the boundary layer has thickened to occupy a significant part of the shock layer while the inviscid part experiences incomplete relaxation of its dissociation chemistry (Fig. 2). Such an expanded scope of analysis embraces essentially all of the interesting nonequilibrium real-gas efforts on stagnation heat transfer (see Refs. 6 and 7).

The analysis is expedited without loss of the essential nonequilibrium flow thermophysics by introduction of the following simplifying assumptions:

1) As far as heat transfer is concerned, ionization can be neglected, and the gas mixture is approximated by a binary mixture of atoms and molecules with negligible thermal diffusion between them.

2) The vibrational internal energy of the molecules is fully excited.

3) The Prandtl and Lewis numbers are near unity and, like the viscosity-density product, are constant across the shock layer.

4) The chemical reaction effects on the shock-layer velocity profile (via the reciprocal density coefficient of the pressure gradient term in the momentum equation) are small enough for a highly cooled wall to permit taking this profile as a known distribution in the leading approximation.

5) The wall surface is highly cooled ($T_W/T_S \ll 1$) such that the nonequilibrium gas-phase chemistry near the wall is recombination rate dominated.

6) Catalytic recombination of atoms on the body surface is governed by a first-order rate law with negligible heterogeneous back dissociation.[4]

7) The freestream is undissociated and strongly hypersonic.

8) The effects of nonequilibrium dissociation on heat transfer vanish before the so-called shock-slip or wall-slip effects (associated with much lower Reynolds numbers; see Ref. 8) are significant.

B. Formulation

Based on these simplifying assumptions, we now present an approximate analytical theory for nonequilibrium-dissociation effects on stagnation-region heat transfer. Such a flow problem is formulated conveniently in terms of the inviscid velocity gradient parameter β_S and its associated similarity coordinate

$$\eta \equiv \sqrt{\frac{(1+\varepsilon\beta_s)}{\rho_w \propto_w}} \int_0^y \rho \, \mathrm{d}y \tag{14}$$

with $u_e = \beta_S x$ in the stagnation region. Denoting $\mathrm{d}/\mathrm{d}\eta$ by a prime, we have the following equations governing the thermochemistry in the flow[8]:

$$Scf\alpha' + \alpha'' = R(\alpha, \theta) \tag{15}$$

$$Prf\theta' + \theta'' = \left(h_D \big/ \hat{C}_p T_e\right) R(\alpha, \theta) \tag{16}$$

where the subscript e denotes the nonequilibrium conditions at the outer edge of the viscous part of the shock layer. From the preceding assumption 3, the functions f and f' are regarded as known functions from an appropriate solution of the shock-layer momentum equation. The term $R(\alpha, \Theta)$ on the right-hand side of atomic specie conservation equation (15) is the nondimensional net gas-phase recombination rate; for a binary mixture of atoms and molecules undergoing the dissociation-recombination reaction

$$A_2 + X \underset{k_r}{\overset{k_d}{\rightleftarrows}} 2A + X \tag{17}$$

(where A_2, A, and X denote a molecule, atom, and any third body, respectively, and $k_r = k_r' T^\omega$ is the recombination rate), this function is

$$R = \Gamma_G \cdot \left(\frac{T_e}{T_s}\right)^{\omega-2} \times \theta^{\omega-2}\left[\frac{\alpha^2}{1+\alpha} - \frac{C_D}{p_e}(1-\alpha)T^{1,5}(1-e^{-3143/T})e^{-\theta_D/\theta}\right]$$

$$\equiv \Gamma_G \cdot \left(\frac{T_e}{T_s}\right)^{\omega-2} \theta^{\omega-2} G(\alpha, \theta) \tag{18a}$$

where Γ_G is a characteristic local-flow-time/gas-phase-reaction-time ratio (Damköhler number) defined by

$$\Gamma_G \equiv \frac{4k_R' Sc T_s^{\omega-2} p_s^2}{(1+\varepsilon)\beta_s R_u^2} \tag{18b}$$

The function $\theta^{\omega-2}$ represents the temperature profile effect on the recombination rate and preexponential portion of the dissociation rate; because $\omega \sim -1.5$ for air, this effect has a considerable influence on the nonequilibrium behavior across a highly cooled boundary layer. The function $G(\alpha, \theta)$ represents the composition-dependent part of

the net atom reaction rate across the boundary layer and involves a contribution from both the local recombination ($\sim\alpha^2$) and dissociation rates; it vanishes identically when the boundary layer is in equilibrium ($\Gamma_G \to \infty$) but does not in the opposite extreme of chemically frozen flow ($\Gamma_G \to 0$).

The outer boundary conditions on α and θ are enforced right behind the shock; for an undissociated freestream with shock-slip effects neglected, these provide that $\alpha(\eta_{\rm SH}) = 0$ and $\theta(\eta_{\rm SH}) = T_F/T_e$, where $\eta_{\rm SH}$ is the shock location determined by the approximate relation that

$$f(\eta_{\rm SH}) = \sqrt{Re_B(\rho_s \propto_s / \rho_w \propto_w)[\rho_\infty/\rho_s(1+\varepsilon)]U_\infty/\beta_s R_B}$$

(Ref. 8). Along the arbitrarily catalytic, cold impermeable wall surface, $\theta(0) = \theta_W \ll 1$ and $f(0) = 0$ for no thermal slip or velocity. There also is the atomic specie boundary condition

$$\alpha'(0) = \sqrt{\frac{\rho_w \propto_w}{(1+\varepsilon)\beta_s}} \frac{Sc K_w}{\propto_w} \alpha(0) = \Gamma_c \alpha(0) \tag{19}$$

where Γ_C is the characteristic local diffusion time to recombination-time ratio (or heterogeneous Damköhler number) in terms of the atom recombination velocity K_W on the surface. This K_W is a known function of the wall temperature and material, which, in turn, is related to the surface catalytic efficiency γ_C by $\gamma_C \equiv (\pi K_W^2/R_m T_W)^{1/2}$. The boundary condition, Eq. (19), expresses the fact that the rate of diffusion of atoms from the gas is balanced by the rate of catalytic recombination on the wall surface. When $\Gamma_C \to \infty$, the surface is completely catalytic [$\alpha(0) = 0$], whereas in the other extreme, $\Gamma_C = 0$, the surface is noncatalytic and the wall atom diffusion rate at the wall vanishes [$\alpha'(0) = 0$].

When the Newtonian value[1] $\beta_s = R_B^{-1}\sqrt{[2(p_s - p_\infty)/\rho_s]}$ and the foregoing expression for γ_C are introduced, it is possible to reexpress the catalytic parameter Γ_C in the manner given by Eq. (12); likewise, the gas-phase reaction parameter Γ_G of Eq. (18) can be expressed in the form of Eq. (13). Once the foregoing split boundary value problem is solved, the corresponding nondimensional, wall heat-transfer rate can be determined from

$$Q_w = \frac{-Pr(\dot{q}_w/C_p T_e)}{\sqrt{\rho_w \mu_w \beta_s (1+\varepsilon)/2}} = \theta'(0) + Le\left[\frac{h_D \alpha'(0)}{C_p T_e}\right] \tag{20}$$

Clearly, only heat conduction contributes to the heat transfer when the wall is completely noncatalytic [$\alpha'(0) = 0$].

C. Analytical Solution

The solution for the generalized low-Reynolds-number (high-altitude) flow regime of interest here divides the shock layer into an outer vortical inviscid region $\eta_e \le \eta \le \eta_{\rm SH}$ containing the nonequilibrium dissociation behind the bowshock and an underlying boundary-layer-like viscous region $0 \le \eta \le \eta_e$ that contains the recombination-dominated nonequilibrium effects (see Fig. 2). An accurate approximate solution for the surface properties under such arbitrary nonequilibrium conditions now can be obtained as follows. First, we perform a purely formal double integration of Eqs. (15) and (16) with respect to η; after applying the boundary conditions and evaluating C_D in terms of G_e and the viscous-layer edge conditions from Eq (18a), we obtain the relations (see Refs. 8 and 9)

$$\frac{\alpha(0)}{\alpha_F(0)} = \frac{\alpha'(0)}{\alpha'_F(0)} = -\frac{\alpha_e \Gamma_G (T_e/T_s)^{\omega-2}}{(1+\alpha_e)} \vartheta_z(f_e) + \frac{1}{\alpha_e}\Gamma_G \left(\frac{T_e}{T_s}\right)^{\omega-2} [-G_e(\alpha_e, T_e)] \cdot I_D(f_e) \tag{21}$$

$$\theta'(0) = \left[\frac{1-\theta_w}{I_\theta(f_e)}\right] + \frac{h_D \vartheta_\theta(f_e)}{I_\theta(f_e)\vartheta_z(f_e)}\left[1 - \frac{\alpha(0)}{\alpha_F(0)}\right] \tag{22}$$

$$\alpha_F(0) = \frac{\alpha'_F(0)}{\Gamma_c} = [1 + \Gamma_c I_z(f_e)]^{-1}\alpha_e \tag{23}$$

where

$$I_z(f_e) \equiv \int_0^{\eta(fe)} \exp\left(-Sc\int_0^\infty f\,{\rm d}\eta\right){\rm d}n \approx \left(0.47 Sc^{\frac{1}{3}} f_\Omega\right)^{-1} \tag{24}$$

$$\vartheta_z(f_e) \equiv \int_0^{\eta(fe)} \exp\left(-Sc\int_0^\eta f\,{\rm d}\eta\right) \times \left[\int_0^\eta \exp\left(-Sc\int_0^\eta f\,{\rm d}\eta\right) R\,{\rm d}\eta\right]{\rm d}\eta \tag{25}$$

$$I_D \equiv \int_0^{\eta(fe)} \exp\left(-Sc\int_0^\eta f\,{\rm d}\eta\right)\left\{\cdot \int_0^\eta \exp\left(Sc\int_0^\infty f\,{\rm d}\eta\right) \times \left[\frac{1-\alpha_F(\eta)}{1-\alpha_e}\right]\theta_F^{\omega-0.5}\left(\frac{1-e^{-3143/T}}{1-e^{-3143/T_s}}\right) \times \exp[-\theta_D(1-\theta_F)/\theta_F]\,{\rm d}\eta\right\}{\rm d}\eta \tag{26}$$

and where I_θ and ϑ_θ are obtained from Eqs. (24) and (25), respectively, by replacing Sc by Pr in the exponentials, while α_F is the chemically frozen flow solution for arbitrary surface catalycity[4] and θ_F is the corresponding temperature profile. The nonequilibrium reaction effect has been split into two parts: one involving the integral $\vartheta_z(f_e)$, which represents the net (recombination-dominated) reaction rate across the inner boundary layer that would exist if the inviscid flow were in equilibrium, and the other involving the integral $I_D(f_e)$, which represents the effect of the nonequilibrium dissociation rate in the inviscid flow as carried into the boundary layer and modified by the rapidly dropping temperature therein. Also note the values of α_e and T_e appearing here, pertaining to the boundary-layer edge $\eta = \eta_e$, are unknowns to be determined by the nonequilibrium dissociation behavior, as discussed next.

Second, we take advantage of a very detailed study[9] of the net reaction rate function for highly cooled walls with their catalytic or noncatalytic surfaces, which showed that the recombination-dominated nature of the chemistry leads to the following convenient yet accurate approximation for the reaction rate integral $\vartheta(f_e)$ over the entire range of nonequilibrium behavior:

$$\vartheta_z(f_e) = \left[\frac{1+\alpha_e}{1+\alpha(0)}\right]\left\{\alpha^2(0) I_1 + \frac{2\alpha(0)\alpha'(0)}{0.47 Sc^{\frac{1}{3}}} I_2 + \left[\frac{\alpha'(0)}{0.47 Sc^{\frac{1}{3}}}\right]^2 I_3\right\}\alpha_e^{-2} \tag{27a}$$

where

$$I_1 \equiv \int_0^{\eta(fe)} \exp\left(-Sc\int_0^\eta f\,{\rm d}\eta\right)\left(\cdot \int_0^\eta \exp\left(-Sc\int_0^\eta f\,{\rm d}\eta\right)\theta_F^{\omega-2} \cdot \left\{1 - \exp\left[-\frac{\theta_D}{\theta_F}(1-\theta_F)\right]\right\}{\rm d}\eta\right){\rm d}\eta \tag{27b}$$

$$I_2 \equiv \int_0^{\eta(fe)} \exp\left(-Sc\int_0^\eta f\,{\rm d}\eta\right)\left(\int_0^\eta \exp\left(Sc\int_0^\eta f\,{\rm d}\eta\right)\theta_F^{\omega-2} \cdot \left\{g_z(\eta) - \exp\left[-\frac{\theta_D}{\theta_F}(1-\theta_F)\right]\right\}{\rm d}\eta\right){\rm d}\eta \tag{27c}$$

$$I_3 \equiv \int_0^{\eta(fe)} \exp\left(-Sc\int_0^\eta f\,{\rm d}\eta\right)\left(\int_0^\eta \exp\left(Sc\int_0^\eta f\,{\rm d}\eta\right)\theta_F^{\omega-2} \cdot \left\{g_z^2 - \exp\left[-\frac{\theta_D}{\theta_F}(1-\theta_F)\right]\right\}{\rm d}\eta\right){\rm d}\eta \tag{27d}$$

are known quadratures of the frozen flow solutions that have been evaluated, extensively tabulated,[8,9] and accurately curve fitted by the formulas

$$I_1 = 4.80(0.50/Sc)^{0.45}(T_w/T_s)^{0.80(1+\omega)-1.84} f_\Omega^{-1.35} \quad (28a)$$

$$I_2 = 1.80(0.50/Sc)^{0.12}(T_w/T_s)^{0.63(1+\omega)-1.15} f_\Omega^{-0.36} \quad (28b)$$

$$I_3 = 0.93(0.50/Sc)^{0.22}(T_w/T_s)^{0.41(1+\omega)-0.65} f_\Omega^{0.66} \quad (28c)$$

valid over the combined parameter range $0.04 \le T_W/T_S \le 0.50$, $-2 \le \omega \le 0$ including the vorticity interaction effect f_Ω. Correspondingly, the "dissociation carryover" integral (26) can be approximately represented by the analytical expression

$$I_D = \frac{2.55\exp\{-0.117[1 - T_w/T_e](T_D/T_e)\}}{\sqrt{[1 - T_w/T_e]T_D/T_e}} \quad (29)$$

Substitution of Eqs. (27–29) into Eq. (21) then yields a simple quadratic equation for the surface nonequilibrium atom concentration with arbitrary Γ_C; denoting $K_D \equiv \Gamma_G(T_e/T_S)^{\omega-2}$ $[\sim G(\alpha_e)]I_D/\alpha_e = I_D/f_4$ with $\alpha_F(0) = \alpha_{Fw} = \alpha_e/(1+\tilde{\Gamma}_c)$, the solution to this equation yields

$$Z = \frac{\alpha(0)}{\alpha_{F_w}} = \frac{\sqrt{\left[1+(1+K_D)\alpha_{F_w}\right]^2 + 4(1+K_D)\Gamma^*} - \left[1-(1+K_D)\alpha_{F_w}\right]}{2\left(\alpha_{F_w}+\Gamma^*\right)} \quad (30)$$

where

$$\Gamma^* \equiv \alpha_e\left[\frac{I_1 + 2\tilde{\Gamma}cI_2 + \tilde{\Gamma}_c^2 I_3}{(1+\tilde{\Gamma}_c)^2}\right]\Gamma_G\left(\frac{T_e}{T_s}\right)^{\omega-2} \quad (31)$$

is a composite Damköhler number representing the simultaneous effects of the finite gas-phase and surface reaction rates, as well as the influence of wall temperature and all of the thermochemical properties of the gas.

Aside from the factor K_D representing an explicit low-Reynolds-number effect, the evaluation of the wall property solution equation (30) requires the determination of the nonequilibrium inviscid properties α_e and T_e. This can be done by solving Eq. (15) with diffusion neglected across the region $\eta_e \le \eta \le \eta_{SH}$ as given in Ref. 8; under the strongly hypersonic flight conditions of interest here and introducing $C_D = C_E p_e$, this yields the following analytical relations:

$$\int_0^{\alpha_e} \frac{d\alpha}{(T/T_s)^{\omega-2}G} = \Gamma_G \cdot f_4 \quad (32)$$

$$(9+\alpha_e)T_e = 9T_F - 2h_D\alpha_e/R_m \quad (33a)$$

where

$$f_4 \equiv [(1+\varepsilon)/2Sc]\,\ell n[(f_1-1)(f_3+1)/(f_1+1)(f_3-1)] \quad (33b)$$

With the foregoing in hand, the corresponding nonequilibrium heat transfer can now be evaluated by the substitution of $\alpha(0) \equiv Z\alpha'_F(0)$ and Eqs. (22) and (23) into Eq. (20). Based on the reference value

$$(I_\theta Q_w)_{EQ} = (1 - T_w/T_s)\hat{C}\,p_{wEQ}T_s + Le^{0.52}h_D\alpha_s \quad (34)$$

pertaining to assumed equilibrium throughout the shock layer, we thus find after some algebra and the use of the inviscid energy equation (33a) the following heat-transfer ratio relationship:

$$\frac{Q_w}{(Q_w)_{EQ}} \approx 1 - \left[\frac{H_D}{1 - T_w/T_s + \alpha_s H_D}\right] \times \left\{0.52(Le-1)(\alpha_s - \alpha_e) + \left[\frac{a_e Z}{1+\tilde{\Gamma}_c}\right][1 - 0.15(Le-1)\tilde{\Gamma}c]\right\} \quad (35)$$

where Z is the nonequilibrium-effect function given by Eq. (30). Equation (35) clearly indicates that low-to-moderate wall catalysis rates can have a large effect on highly cooled wall heat transfer when the shock layer is dissociated and well out of gas-phase equilibrium.

IV. Summary of Working Relationships

The foregoing analysis provides accurate closed-form solutions for the nonequilibrium flow properties at the viscous-layer edge and the atom concentration and heat transfer on the surface that include arbitrary degrees of both surface catalycity and recombination-dominated nonequilibrium flow across the boundary layer. The former properties α_e, T_e are governed by Eq. (32) and (33). Based on the input parameters of Sec. II, these equations can be solved by a method of the users choice for α_e and T_e on the ranges $0 \le \alpha_e \le \alpha_S$, $T_S \le T_e \le T_F$, respectively. Once this is done, the inviscid reaction-rate carryover effect integral I_D is calculated from Eq. (29), and the atom concentration mass fraction at the wall can then be determined for any desired values of Γ_G and Γ_C from Eqs. (30) and (31).

The corresponding result for the heat transfer, Eq. (35), is the desired working equation that describes the nonequilibrium effects relative to the equilibrium-dissociated value pertaining to the same flight/body conditions. We note that Eq. (35) encompasses the entire extent of nonequilibrium/finite-wall catalycity effects depending on the individual values of the two Damköhler number parameters Γ_G and Γ_C, respectively. For example, the limit $\Gamma_G \gg 1$ corresponds to equilibrium-dissociation behavior throughout the boundary layer giving $Z \to 0$ and hence $q_w \to q_{w,EQ}$. The opposite limit $\Gamma_G \to 0$ pertains to a chemically frozen (nonreacting) boundary layer with $Z \to 1$, giving a heat-transfer rate that is highly dependent on the degree of finite-wall catalycity reflected in the prevailing value of Γ_C. The closed form of the foregoing analysis provides not only valuable physical insight but also a very efficient computational model of how various design parameters influence the relative nonequilibrium effect on heat transfer. In particular, it can be used as an interpolative relationship between any frozen and equilibrium heat-transfer solution routines the user wishes to supply. In the present work, we have used analytical values, but it is emphasized that purely numerical values from any appropriate aerodynamic heating code would serve equally well.

V. Validation

As discussed in Ref. 3, predictions obtained from the foregoing theory in the higher-Reynolds-number regime of equilibrium inviscid flow have proven to be in excellent agreement with several exact numerical solutions of the stagnation boundary-layer equations over a wide range of both gas-phase nonequilibrium state Γ_G and surface catalycity Γ_C. An example is shown here in Fig. 3, where the close agreement (within 5 to 10%) with Fay and Riddell's well-known results[1] for the complete nonequilibrium boundary-layer regime is illustrated. Another application is illustrated in Fig. 4, where the nonequilibrium heat transfer vs altitude is shown for a typical case as a function of various assumed values of the wall catalytic efficiency. The resulting significant reduction in heating predicted by the present theory for moderately to weakly catalytic walls is seen to be in excellent agreement with Chung's[7] exact numerical solutions up to 64 km (210 kft) altitude.

Concerning the additional high-altitude effects of the inviscid nonequilibrium flow incorporated here, an appreciation of the present theory's typical accuracy can be obtained from Fig. 5, where the predicted heat-transfer ratio $Q_w/Q_{w,EQ}$ is plotted vs altitude for a perfectly noncatalytic axisymmetric body with $R_B = 0.3$ m (1 ft) flying at 7.9 km/s (26 kft/s) in the undissociated standard atmosphere. To bring out the various physical effects involved, there is also indicated the result obtained assuming an equilibrium inviscid flow and that obtained by neglecting the inviscid reaction carryover effect connected with the term I_D. It is seen that the present theory agrees well with the exact numerical solution of Chung (also shown) throughout the entire nonequilibrium flow regime, underestimating the effect of shock-layer reaction on heat transfer by no more than

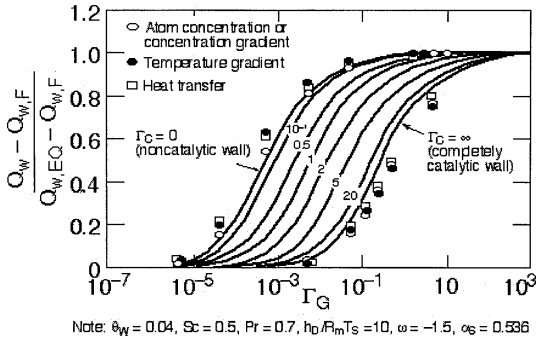

Fig. 3 Comparison of present theory with exact numerical solutions of Fay and Riddell.

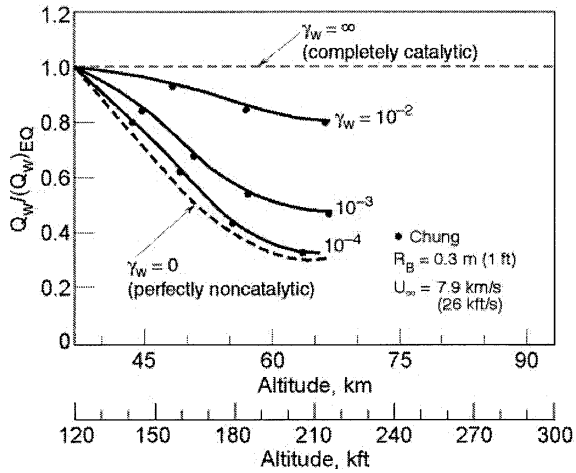

Fig. 4 Predicted effect of catalytic efficiency on the altitude variation of nonequilibrium heating.

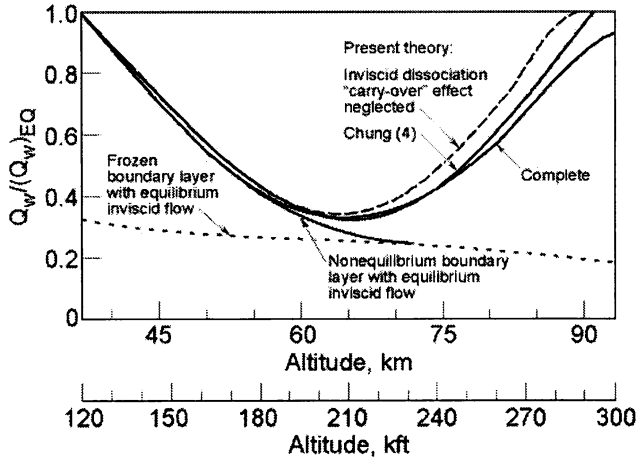

Fig. 5 Nonequilibrium stagnation point heat transfer: U_∞ = 26,000 ft/s, R_B = 1 ft, Le = 1, noncatalytic surface.

10%. However, this agreement is noticeably improved when the explicit inviscid reaction carryover effect is included, which causes a reduced prediction of heat transfer at the lower densities corresponding to dissociation ratecontrolled shock-layer flow.

Further corroboration of the present theory can be found in a comparison with the more recent viscous shock-layer solution results of Zoby et al.,[10] as shown in Fig. 6. When adjusted for the different recombination-rate temperature-dependence exponents used, we obtain predictions of the typical noncatalytic heat-transfer rate that agree reasonably well with those of Ref. 10 over a significant range of altitudes.

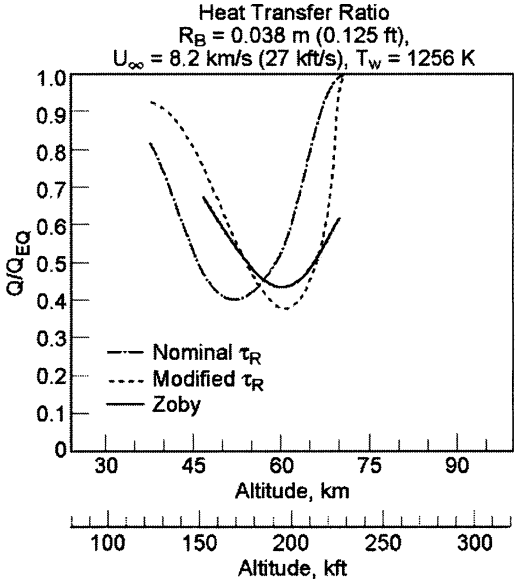

Fig. 6 Comparison of present theory and viscous shock-layer computations.

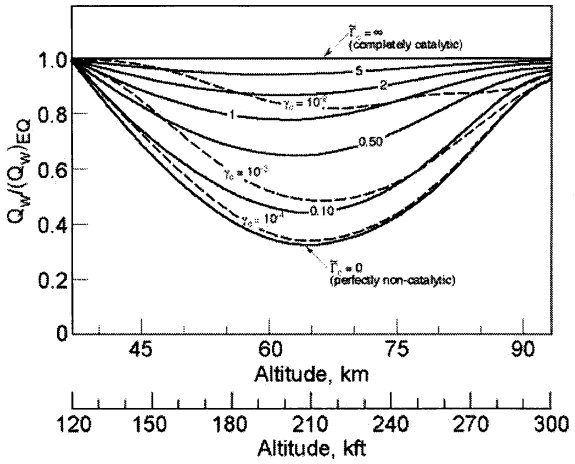

Fig. 7 Effect of surface catalycity on nonequilibrium heat transfer.

VI. Finite Surface Catalysis Effects

The present theory provides an efficient means of assessing the effect of an arbitrary amount of finite-surface catalysis on nonequilibrium stagnation heating over the complete range of altitude/flight speed conditions. An example in terms of the basic catalytic Damköhler Γ_C is shown in Fig. 7. It is seen that the influence of gas-phase reaction is very sensitive to the surface catalycity when the shock layer is appreciably out of equilibrium and significantly dissociated. This sensitivity is greatest when the boundary layer is chemically frozen while the inviscid flow is essentially in equilibrium; however, it persists well into the lower-Reynolds-number regime of completely inviscid dissociation rate-controlled flow.

In connection with these general results, it is of interest to indicate what actual degrees of surface catalycity and heat transfer can be expected for various surface materials. Accordingly, Γ_C and the corresponding heat transfer were evaluated as a function of altitude assuming $\gamma_C = 10^{-2}$ (typical of metallic oxides) and 10^{-3} and 10^{-4} (typical of glassy-type materials such as Pyrex); the results are also indicated on Fig. 7 by the dashed curves. It is seen that blunt bodies having a metallic-type surface behave as very nearly perfectly catalytic throughout most of the nonequilibrium flight regime in this example and consequently experience virtually the full equilibrium stagnation heating level regardless of altitude. Here, the body surface tends to act in a perfectly noncatalytic manner only at very high altitudes where little dissociation occurs in the shock layer. In sharp

contrast, glassy-type surfaces having catalytic efficiencies of the order of 10^{-2} or less behave as though they were noncatalysts under the same flight conditions. They, therefore, experience stagnation heat-transfer rates substantially lower than the equilibrium value throughout the altitude range 46–82 km (150–270 kft). Clearly, the choice of surface materials from the standpoint of their surface catalytic efficiency has an important bearing on convective heating of hypervelocity vehicles that spend appreciable time at high altitudes.

VII. Parametric Studies

The present theory provides a very computationally efficient and inexpensive tool for conducting parametric sensitivity and design tradeoff studies of thermal protection systems. Results of the former pertaining to the lower-altitude boundary layer with equilibrium inviscid flow have in fact been given earlier including assessment of the sensitivity to both gas-phase and catalytic surface chemical rate data.[5] The extended treatment to further include the higher-altitude nonequilibrium inviscid flow aspect now provides a capability to carry out design-parameter and flight-condition sensitivity studies over the full range of high to low altitudes. An example is given in Fig. 8, which shows the influence of nose radius on the relative

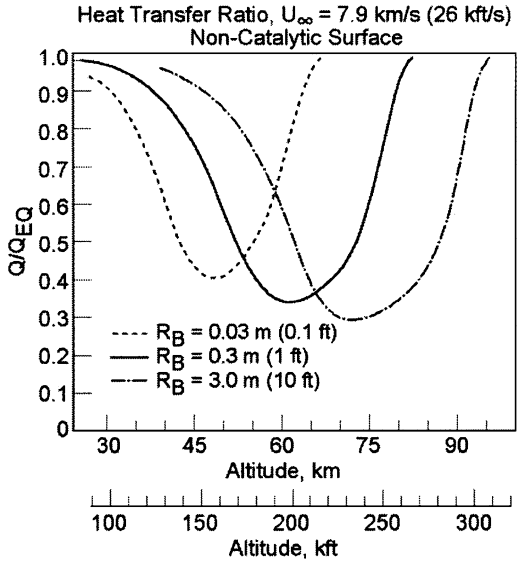

Fig. 8 Variation of nonequilibrium heat-transfer ratio with altitude for three different nose radii.

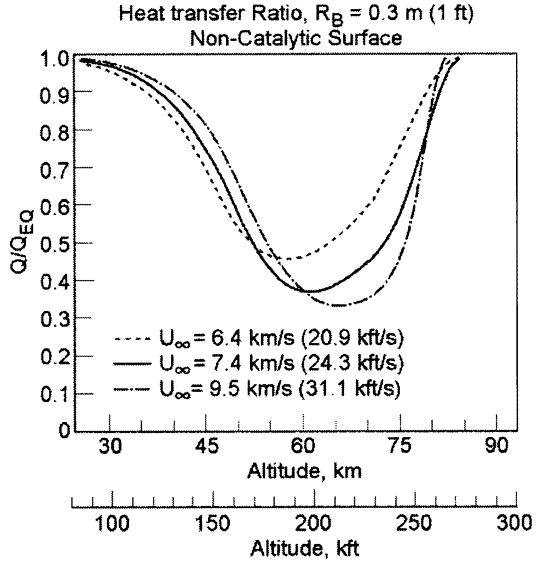

Fig. 9 Variation of nonequilibrium heat-transfer ratio with altitude for three different flight velocities.

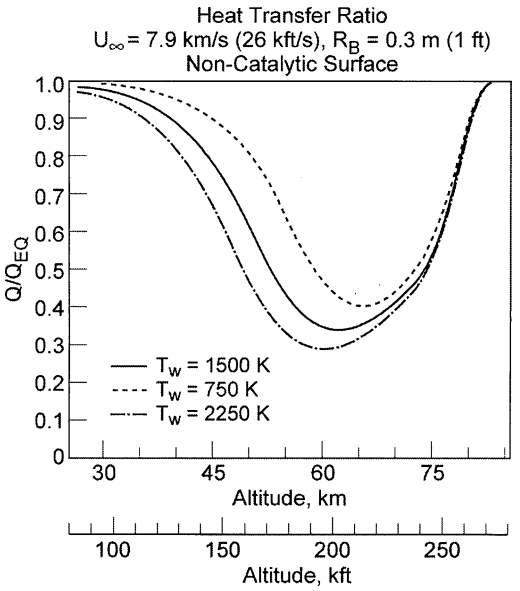

Fig. 10 Effect of wall temperature on nonequilibrium heating.

nonequilibrium heating ratio over the complete altitude range of practical interest for entry vehicle work. Bearing in mind that the usual $\sqrt{R_B}$ dependence of heating has already been accounted for in the ordinate, Fig. 8 clearly illustrates the dramatic enhancement of nonequilibrium chemistry effects because of reduced body size. This feature of the theory has recently found application in the study of orbital spacecraft reentry breakup.[11]

Another example is given in Fig. 9 illustrating the influence of flight velocity for a given body; this influence on the relative nonequilibrium heating effect is seen to be weak, especially in the lower-altitude regime, owing to the fact that the main dependence on U_∞ has already been included in the ordinate ratio. A third and final example is given in Fig. 10, showing the sensitivity to wall temperature: cooling the surface reduces the nonequilibrium effect primarily because of the $T_w^{-3.5}$ dependence of the recombination rate near the wall.[12,13]

VIII. Conclusions

By drawing upon a well-validated approximate theory of reacting viscous shock layer flow on highly cooled bodies, we have presented an analytical method for predicting nonequilibrium dissociation/recombination effects on stagnation heat transfer to arbitrarily catalytic surfaces that yields accurate results over the complete range of hypersonic flight speeds and altitudes where such effects are significant. The theory is especially well suited to rapid engineering predictions along any desired entry trajectory or lifting-vehicle flight path, as well as to cost-effective parametric studies of the influence of various basic gas dynamic or thermodynamic properties.

The results of such an application in the lower altitudes pertaining to an equilibrium inviscid have already been published.[13] The present work would enable an extension of this application to include the range of even higher altitudes when a fully nonequilibrium shock layer occurs.

References

[1]Fay, J. A., and Riddell, F. R., "Theory of Stagnation Point Heat Transfer in Dissociated Air," *Journal of the Aeronautical Sciences*, Vol. 25, No. 2, 1958, pp. 73–85.

[2]Sebo, D. E., "Heating Effects of Multiple Skip Reentry Trajectories," Aerospace Corp., Rept. ATR 91 (6822)-1, El Segundo, CA, May 1991.

[3]Inger, G. R., "Analytical Method for Predicting Nonequilibrium Boundary Layer Heat Transfer with Arbitrary Surface Catalycity," Aerospace Corp., Rept. ATR-94(4822)-1, El Segundo, CA, Oct. 1993.

[4]Goulard, R. J., "On Catalytic Recombination Rates in Hypersonic Stagnation Heat Transfer," *Jet Propulsion*, Vol. 28, No. 11, 1958, pp. 737–745.

[5]Inger, G. R., and Elder, J., "Recombination-Dominated Nonequilibrium Heat Transfer to Arbitrarily-Catalytic Hypersonic Vehicles," *Journal of Thermophysics and Heat Transfer*, Vol. 5, April 1991, pp. 449–455.

[6]Blottner, F., "Viscous Shock Layer at the Stagnation Point with Non-Equilibrium Chemistry," *AIAA Journal*, Vol. 7, No. 12, 1969, pp. 1921–1927.

[7]Chung, P. M., "Hypersonic Viscous Shock Layer on Non-Equilibrium Dissociating Gas," NASA Rept. R-109, May 1961.

[8]Inger, G. R., "Non-Equilibrium Hypersonic Stagnation Flow with Arbitrary Surface Catalycity Including Low Reynolds Number Effects," *International Journal of Heat and Mass Transfer*, Vol. 9, 1966, pp. 755–772.

[9]Inger, G. R., "Non-Equilibrium Stagnation Point Boundary Layers with Arbitrary Surface Catalycity," *AIAA Journal*, Vol. 1, No. 8, 1963, pp. 1776–1783.

[10]Zoby, E. V., Lee, K. P., Gupta, R. N., Thompson, R. A., and Simmonds, A. L., "Viscous Shock-Layer Solutions with Nonequilibrium Chemistry for Hypersonic Flows Past Slender Bodies," *Journal of Spacecraft and Rockets*, Vol. 26, No. 4, 1989, pp. 221–230.

[11]Baker, R. L., Weaver, M. A., Moody, D. M., and Wan, C.-C., "Orbital Spacecraft Reentry Breakup," *Space Debris 1999*, edited by J. Bendisch, Vol. 100, American Astronomical Society Science and Technology Series, Univelt, San Diego, CA, 2001, pp. 365–378.

[12]Inger, G. R., "Correlation of Surface Temperature Effect on Nonequilibrium Heat Transfer," *ARS Journal*, Vol. 32, No. 11, 1963, pp. 1743–1744.

[13]Gnoffo, P. A., and Inger, G. R., "Analytical Corrections to Computational Heating Predictions Accounting for Changes in Surface Catalysis," *Journal of Spacecraft and Rockets*, Vol. 35, No. 4, 1998, pp. 417–423.

T. Lin
Associate Editor